Research Square

Preprints are preliminary reports that have not undergone peer review.
They should not be considered conclusive, used to inform clinical practice,
or referenced by the media as validated information.

Ultrasonic–microwave-assisted impregnation of aspen wood with waterborne epoxy resin: process-structure-property relationships

Xinhao Feng
fengxinhao@njfu.edu.cn
Nanjing Forestry University
Yuehan Sun
Nanjing Forestry University
Tingting Peng
Nanjing Forestry University
Zhaozhe Yang
Chinese Academy of Forestry
Jian Chen
Chinese Academy of Forestry
Guomin Wu
Chinese Academy of Forestry
Zhihui Wu
Nanjing Forestry University

Research Article

Keywords:

Posted Date: September 4th, 2026

DOI: https://doi.org/10.21203/rs.3.rs-10833968/v1

License: This work is licensed under a Creative Commons Attribution 4.0 International License.
Read Full License

Additional Declarations: No competing interests reported.

Abstract

Efficient impregnation and environmentally compatible modifiers are essential for improving the performance and sustainability of wood modification. In this study, an ultrasonic-microwave synergistic (UMS) impregnation strategy was combined with waterborne epoxy resin (WEP) to enhance resin penetration and improve the physical, mechanical, and thermal properties of Canadian aspen (*Populus tremuloides*). Wood samples were treated with WEP solutions at concentrations of 0%, 5%, 15%, and 25%, followed by vacuum-assisted impregnation, drying, and thermal curing. Increasing the WEP concentration progressively increased resin retention and density, with a weight percent gain of 39% and a density increase from 0.41 to 0.49 g/cm³ at 25% WEP. WEP modification substantially reduced water absorption and improved dimensional stability, resulting in maximum reductions of 45% in radial swelling and 30% in tangential shrinkage. The flexural strength increased to 115 MPa, representing an improvement of 29% compared with unmodified wood, while cross-sectional hardness and surface hydrophobicity were also enhanced. Chemical analyses revealed changes in the chemical environment associated with WEP curing and wood-resin interactions, whereas thermogravimetric analysis demonstrated improved thermal stability. Structural observations showed a concentration-dependent transition from an open cellular structure to one containing progressively more WEP-rich layers and locally resin-filled regions. The enhanced performance was attributed to the combined effects of UMS-assisted treatment, in situ curing and retention of WEP within the wood structure, and interfacial interactions between the cured resin and wood components. Overall, the coupling of UMS process intensification with WEP system provides an efficient and environmentally approach for producing durable, high-performance modified wood.

Introduction

Wood is a renewable bio-based material with a hierarchical cellular architecture, favorable specific mechanical properties, and broad applications in construction, furnishings, packaging, and other engineering fields. Nevertheless, wood is intrinsically porous and hygroscopic because its cell-wall polymers contain abundant hydroxyl groups and its anatomical structure contains interconnected vessels, pits, and other transport pathways. The uptake and release of water induce anisotropic swelling and shrinkage and can consequently cause dimensional instability, cracking, deformation, and deterioration of long-term service performance. Wood modification technologies have therefore been extensively investigated to regulate wood-water interactions and improve dimensional stability, durability, mechanical performance, and functional properties (Brischke and Alfredsen 2020; Sandberg et al. 2017; Thybring et al. 2018; Xie et al. 2013; Zelinka et al. 2022).

Wood modification can be broadly achieved through chemical reactions, thermal treatment, impregnation, and combinations of physical and chemical processes (Sandberg et al. 2017; Zelinka et al. 2022). Among these approaches, chemical and impregnation modifications are particularly effective because they can reduce the accessibility of moisture-sensitive groups, introduce hydrophobic or dimensionally stable components, and form polymeric phases within the hierarchical wood structure

(Mantanis 2017; Xie et al. 2013). Acetylation, for example, substitutes accessible hydroxyl groups with acetyl groups and thereby alters the interactions between wood and water (Chang and Chang 2002; Digaitis et al. 2021; Mantanis 2017). Furfurylation introduces furfuryl alcohol into wood, followed by its polymerization within the cell wall and cellular voids, resulting in improved dimensional stability and durability (Mantanis 2017; Yang et al. 2019). Other impregnation systems, including rosin and water-soluble vinyl monomers, have also been used to reduce water uptake and reinforce fast-growing wood (Dong et al. 2016; Huang et al. 2019). However, increasing environmental concerns and restrictions on volatile organic compounds have stimulated interest in aqueous or lower-solvent modification systems that can provide effective fixation and property enhancement without extensive dependence on organic carriers (Mantanis 2017; Sandberg et al. 2017; Zelinka et al. 2022).

Waterborne epoxy resin (WEP) is a promising modifier because it combines aqueous processability with the adhesion, chemical functionality, mechanical performance, and cross-linking capability of thermosetting epoxy resins. Compared with conventional solvent-based epoxy formulations, water serves as the principal dispersion medium in WEP systems, potentially reducing the use and emission of organic solvents during preparation and impregnation. After water removal and thermal curing, WEP can form a cross-linked polymer network within accessible wood structures and may interact with hydroxyl-containing wood components through chemical and physicochemical interactions. Wang et al. (2021) demonstrated that in situ cross-linking of WEP within wood improved its dimensional stability, thermal stability, and decay resistance. Sun et al. (2021) combined sodium silicate and WEP to improve the water resistance, dimensional stability, and mechanical performance of Chinese fir, whereas Hao et al. (2022) used ammonium polyphosphate and WEP to prepare high-strength, dimensionally stable, and flame-retardant poplar. These findings establish WEP as a potentially effective aqueous polymer system for the high-performance modification of wood.

The effectiveness of WEP modification, however, depends not only on resin chemistry and curing behavior but also on the transport, distribution, and retention of the aqueous resin dispersion within wood. Wood permeability is strongly influenced by species, density, moisture condition, anatomical direction, vessel connectivity, pit aspiration, extractive deposition, and the dimensions of the modifier particles. Consequently, conventional soaking or vacuum-pressure impregnation may result in slow and spatially heterogeneous modifier transport, particularly in wood with poorly accessible transverse pathways. Increasing the resin concentration may enhance total resin uptake but can also increase viscosity, particle aggregation, and accumulation in surface or near-surface regions. Therefore, physical process-intensification methods that improve liquid movement and increase the accessibility of anatomical transport pathways may be needed to achieve more effective WEP impregnation.

Ultrasonic treatment has been investigated as a physical means of intensifying liquid transport in wood. The propagation of ultrasound through a liquid produces pressure oscillations, acoustic streaming, and cavitation, which can enhance fluid agitation and interfacial mass transfer. Under appropriate treatment conditions, cavitation-related forces may also disturb pit membranes, parenchyma cells, or weak anatomical regions and thereby create additional pathways for liquid penetration. Liu et al. (2015)

reported that ultrasonic-assisted treatment improved dye uptake in wood veneer by enhancing permeability and generating additional transport and sorption sites. Wang et al. (2018) similarly demonstrated that ultrasonic parameters affected reactive-dye penetration and fixation in fast-growing poplar. These studies indicate that ultrasound can promote the movement of aqueous modifiers through wood, although the outcome depends strongly on ultrasonic power, treatment time, liquid properties, specimen dimensions, and wood anatomy.

Microwave treatment provides a different but potentially complementary mechanism for improving wood impregnation. Because microwave energy interacts strongly with polar components, particularly water, microwave irradiation can produce rapid volumetric heating and internal vapor-pressure gradients within moist wood. When the generated internal pressure exceeds the resistance of weak anatomical structures, pit membranes, ray tissues, middle-lamella regions, or other flow-restricting structures may be opened or locally disrupted, thereby increasing liquid permeability. He et al. (2014) reported that microwave treatment substantially enhanced the liquid permeability of Chinese fir. Xu et al. (2015) showed that microwave pretreatment increased the transverse permeability and resin impregnation weight gain of poplar wood. Microscopic observations by Terziev et al. (2020) further revealed changes in pit membranes and other anatomical structures following intensive microwave treatment, while Weng et al. (2021) demonstrated that controlled microwave pretreatment accelerated the drying of thick Chinese fir lumber. These results demonstrate the potential of microwave processing to improve internal moisture movement and modifier transport, although excessive microwave severity may produce undesirable cracking or reductions in mechanical performance.

The distinct mechanisms of ultrasound and microwave treatment suggest that their integration may provide complementary effects during wood impregnation. Ultrasound primarily enhances liquid-phase movement, interfacial mass transfer, and local fluid penetration, whereas microwave irradiation induces rapid internal heating and pressure-driven transport within the moist wood structure. Combined microwave-ultrasonic processing has been used to intensify heat and mass transfer during lignocellulosic biomass conversion. Lu et al. (2016), for example, reported that microwave-ultrasonic-assisted liquefaction accelerated the conversion of woody biomass while reducing processing time and solvent consumption. More broadly, ultrasound has been recognized as an effective process-intensification tool for the conversion and treatment of lignocellulosic materials (Flores et al. 2021). Nevertheless, most combined ultrasonic-microwave studies have focused on biomass extraction, liquefaction, or chemical conversion rather than on the impregnation modification of bulk wood. The relationships among combined ultrasonic-microwave treatment, WEP uptake and distribution, modification of the cellular structure, and the resulting macroscopic performance therefore remain insufficiently understood.

Accordingly, this study investigated the modification of Canadian aspen (*Populus tremuloides*) with WEP using an ultrasonic-microwave synergistic impregnation process. In the present work, the term “synergistic” refers to the integrated use of ultrasonic and microwave treatments to exploit their complementary effects on liquid-phase transport and internal heating rather than to a quantitatively

demonstrated interaction between separately evaluated treatments. It was hypothesized that the combined physical treatment would facilitate the transport of the aqueous WEP system through accessible anatomical pathways, while subsequent vacuum treatment, drying, and thermal curing would retain and polymerize WEP within the hierarchical wood structure. WEP concentration was varied from 0 to 25% to establish relationships among resin uptake, physical properties, dimensional stability, mechanical and surface performance, thermal behavior, chemical characteristics, and microstructural evolution. Weight percent gain, density, water absorption, swelling and shrinkage, anti-swelling and anti-shrinkage efficiencies, hardness, flexural strength, water contact angle, and surface color were evaluated. Fourier transform infrared spectroscopy, thermogravimetric analysis, X-ray diffraction, X-ray photoelectron spectroscopy, and scanning electron microscopy were further used to elucidate the chemical, thermal, and microstructural changes induced by WEP modification. This work aims to provide an aqueous, lower-solvent approach for improving wood performance and to clarify the process-structure-property relationships governing ultrasonic–microwave-assisted WEP impregnation.

Materials and Methods

Materials

Canadian aspen (*Populus tremuloides*) boards with dimensions of 1500 × 200 × 30 mm^3 (L × R × T) were supplied by FPInnovations (Alberta, Canada). All wood samples were conditioned at 20 ± 2 ℃ and 65 ± 3% for 48 h before further testing. The waterborne epoxy resin (WEP) was self-synthesized in the lab as described in previous study (Yang et al. 2024). It is a milky-white aqueous dispersion with a solid content of 49 wt%, a viscosity of 260 mPa • s at 25°C, and an average particle size of 488 nm. Diethyltoluene diamine (DETDA; Aladdin Chemical Reagent Co., Ltd., Shanghai, China) was used as the curing agent at a WEP-to-DETDA mass ratio of 10:1. All chemicals were used without any further purification.

Process of Wood Modification

The wood modification process consisted of preparation of the impregnation solutions, ultrasonic-microwave-assisted impregnation, subsequent vacuum treatment, staged drying, and thermal curing. Aqueous impregnation solutions containing 0%, 5%, 15%, and 25% WEP were prepared by diluting the WEP dispersion with deionized water. DETDA was then added at a WEP-to-DETDA mass ratio of 10:1. Each mixture was ultrasonicated for 5 min and subsequently magnetically stirred for 5 min to obtain a homogeneous impregnation solution.

The wood specimens were completely immersed in the corresponding impregnation solution and treated in an ultrasonic-microwave synergistic reaction workstation (XO-SM100, ATPIO Co., Ltd., Nanjing, China). The integrated treatment used in this study consisted of sequential ultrasonic and microwave treatment. Ultrasound was first applied at a nominal power of 1000 W for 10 min. Microwave treatment was

subsequently conducted at a nominal power of 1000 W, during which the temperature of the impregnation solution was increased to 90°C and maintained at this temperature for 20 min.

Following ultrasonic-microwave treatment, the specimens remained immersed in the impregnation solution and were subjected to vacuum treatment for 24 h to further promote resin uptake. The impregnated specimens were then removed from the solution and air-dried for 48 h, followed by staged oven drying at 40°C for 2 h, 80°C for 2 h, and 103°C for 1 h. Finally, the dried specimens were thermally cured at 170°C for 2 h to promote polymerization and fixation of WEP within the wood structure. The treatment groups were designated according to the WEP concentration of the impregnation solution as 0%, 5%, 15%, and 25%. Eight independent specimens were prepared for each treatment condition.

Measurements and Characterizations

The weight percent gain (WPG) and density of modified samples were calculated by measuring the weight and volume of samples before and after modification. The dimensional stability of modified sample was examined by swelling/shrinkage rate and anti-swelling/shrinkage efficiency (ASE) in the radial, tangential, and volume direction according to Chinese standard of GB/T 1927.6–2021 and GB/T 1927.8–2021, respectively. Simultaneously, the water absorption and dried volume bulking were also obtained by the weight and volume variation before and after water soaking for 0.5 h, 1 h, 2 h, 4 h, 34 h, 56 h, 105 h, and 165 h, according to Chinese standard of GB/T 1927.7–2021.

The hardness and flexural strength of sample were tested using a universal mechanical tester (Model 5567, Instron Inc. MA, USA) according to Chinese standard of GB/T1927.19-2021 and GB/T1927.9-2021, respectively. During the hardness testing, the semi-spherical steel indenter with diameter of 11.28 mm was pressed into wood sample (50 × 50 × 50 mm^3, L × R × T) by 5.64 mm in depth at the loading rate of 3 mm/min, and the ending load was recorded as the hardness of sample. For the flexural testing, the sample with dimension of 300 × 20 × 20 mm^3 (L × R × T) was tested in three-point bending model at the loading rate of 5 mm/min. Eight duplicates were tested in every condition of both testing.

Water contact angle of the samples was measured with a contact angle goniometer (DSA 100, Kruss Ltd., Germany) at room temperature. 10 μL distilled water was directly pumped from a micro-syringe onto the surface of samples and the instant image was captured using a telescope equipped with a video camera. The results were obtained by the average value of six independent measurements on each sample.

The surface color of samples was measured using a handheld spectrophotometer (Ci60, X-Rite, Shanghai, China) to explore color variation before and after modification according to the CIE-L*a*b* system (Hunt 2002). In the system, three parameters, L*, a*, and b* that represent the brightness, red/green color pair, and yellow/blue color pair, respectively, were collected and the total color difference (ΔE*) was calculated according to the equation below.

$$\Delta E^* = \sqrt{\left(L^* - L_0^*\right)^2 + \left(a^* - a_0^*\right)^2 + \left(b^* - b_0^*\right)^2}$$

1

where L^*, a^*, and b^* represent the color parameters of the sample after modification, and L_0^*, a_0^*, and b_0^* represent the color parameters without modification.

The WEP resin and thin layer of wood sample was placed in Fourier transform infrared spectroscopy (VERTEX 80 V, Bruker, Karlsruhe, Germany) to analyze the functional groups and their changes before and after curing or modification, respectively. The sample was tested under a scanning range from 400 to 4000 cm^{-1}, with a resolution of 4 cm^{-1} by an Attenuated Total Reflectance method.

The thermal stability of modified sample was evaluated by a thermal gravimetric analyzer (STA 409 PC, NETZSCH, Selb, Germany) at the temperature from 25 to 600 ℃ with a heating rate of 10 ℃/min in the nitrogen atmosphere.

The effect of modification on the wood crystallinity was performed in an X-ray diffractometer (D8 ADVANCE, Bruker, Karlsruhe, Germany) using Cu target radiation (λ = 1.54 Å). The acceleration voltage was 40 kV, the scan range (2θ) was 5°-40° at a rate of 2 °/min, and the tube current was 30 mA.

The surface chemical composition of modified wood was analyzed by an X-ray photoelectron spectroscopy (AXIS Ultra DLD, Osaka, Japan). A low-resolution scan from 0 to 1100 eV binding energy was used to determine the concentration of surface elements along with the change of oxygen to carbon (O/C) atomic ratio, and a high-resolution scan of the C1s region from 277 to 300 eV at a pass energy of 50 eV was also recorded to further analyze the chemical bond in the oxygen and carbon atoms.

The surface morphology of samples before and after modification was observed with a scanning electron microscopy (QUANTA 200 FEI, OR, USA) at the accelerating voltage of 2 kV. The cross-section of sample was prepared by freezing and breaking the sample in liquid nitrogen, and prior to SEM testing, the samples were sprayed with a thin layer of gold (AU) in order to improve their electrical conductivity.

Results and discussion

Physical properties

The uptake and retention of WEP within the wood structure were first evaluated by weight percent gain (WPG), density, volume bulking, and water absorption (Fig. 1a). The WPG increased with increasing WEP concentration and reached approximately 39% at 25% WEP. Only a limited change in WPG was observed after water soaking for 165 h, indicating that a substantial proportion of WEP was retained within the wood after thermal curing and water soaking. Similar results have been observed for WEP-impregnated wood, where curing of the resin within the porous wood structure contributed to improved resistance to water and dimensional changes (Hao et al. 2022; Sun et al. 2021; Wang et al. 2021).

The density exhibited a trend similar to that of WPG (Fig. 1b), increasing from 0.41 g/cm³ for the unmodified wood to 0.49 g/cm³ at 25% WEP. This increase primarily resulted from the retention and curing of WEP within the wood structure. The density measured after the water soaking procedure was slightly higher than that before soaking. This result can be associated with the volume reduction in the dry specimen after the soaking-drying cycle, because density is determined by the relative changes in both mass and volume. As shown in Fig. 1c, part of the initial volume bulking generated by WEP modification was lost after water soaking, with the relative reduction increasing from 41% to 47% as WEP concentration increased. This decrease may arise from the removal of water-soluble extractives and loosely retained fractions together with irreversible rearrangement or shrinkage of the wood structure during the wetting-drying cycle (Bastani et al. 2015; Roffael 2016). Nevertheless, the stable WPG after soaking indicates that most of the cured WEP retained within the wood.

WEP modification altered the water-uptake behavior of the wood (Fig. 1d). The water absorption of the WEP-modified specimens was lower than that of the 0% WEP and decreased with increasing WEP concentration. The difference was evident during the initial stage of immersion, when the 0% WEP-treated wood absorbed water more rapidly than the WEP-modified specimens. The initial water-absorption process in wood is strongly influenced by accessible capillary pathways and hydrophilic sites. The cured WEP associated with internal wood surfaces and locally occupying cellular voids can reduce the effective continuity and volume of pathways available for liquid-water transport while simultaneously changing the chemical environment of accessible wood surfaces. In situ formation of WEP networks within wood has been reported to reduce water uptake and improve dimensional stability (Sun et al. 2021; Wang et al. 2021).

Overall, the physical-property results demonstrate that increasing WEP concentration promoted resin retention and restricted water absorption into the wood. These effects provide the first macroscopic evidence that the ultrasonic-microwave-assisted impregnation process successfully introduced the WEP into accessible regions of the hierarchical wood structure.

Dimensional stability

WEP modification improved the dimensional stability of the wood, as demonstrated by the swelling, shrinkage, and anti-swelling/shrinkage efficiency results in Fig. 2. The swelling and shrinkage in the radial and tangential directions and on a volumetric basis generally decreased with increasing WEP concentration (Fig. 2a, b). At 25% WEP, the maximum reductions relative to the 0% WEP reference reached approximately 45% for radial swelling and 30% for tangential shrinkage.

The anisotropic dimensional response is associated with the hierarchical structure of the wood cell wall and the different anatomical constraints in the radial and tangential directions (Elaieb et al. 2019; Li et al. 2025). WEP modification did not eliminate this intrinsic anisotropy but reduced the magnitude of moisture-induced dimensional changes. The corresponding anti-swelling and anti-shrinkage efficiencies increased with WEP concentration (Fig. 2c, d), with maximum values of approximately 30% observed in the radial and tangential directions at 25% WEP.

The improvement in dimensional stability can be explained by several mutually reinforcing mechanisms. Firstly, the cured WEP within wood reduced the amount and continuity of accessible pathways available for rapid liquid-water transport, as supported by the lower water absorption in Fig. 1d. Secondly, the cured polymer associated with internal cell surfaces and locally occupied cellular voids could mechanically constrain the deformation of the surrounding wood structure during moisture uptake and release. Thirdly, interactions between the cured WEP and hydroxyl-containing wood components may reduce the effective accessibility of hydrophilic sites. Previous studies on WEP-modified wood also demonstrated that in situ cross-linking or retention of WEP within wood can substantially improve dimensional stability and water resistance (Hao et al. 2022; Sun et al. 2021; Wang et al. 2021).

The dimensional-stability results therefore agree well with the physical-property trends in Fig. 1. Greater WEP retention at higher concentrations was accompanied by lower water absorption and reduced swelling and shrinkage. Nevertheless, the anti-swelling and anti-shrinkage efficiencies did not increase in direct proportion to WPG, indicating that the effectiveness of the introduced resin depended not only on its total amount but also on its spatial distribution and interaction with the moisture-responsive wood structure. This concentration-dependent distribution is further supported by the XPS and SEM observations discussed below.

Mechanical and surface properties

The effect of WEP modification on wood hardness was strongly dependent on the anatomical surface tested (Fig. 3a). The hardness measured on the radial and tangential surfaces changed only slightly with increasing WEP concentration, whereas the cross-sectional hardness increased progressively. This anisotropic response is likely associated with the distribution of WEP along the longitudinally oriented cellular structure of the wood. As subsequently shown by SEM, WEP was deposited on internal lumen-facing surfaces and locally accumulated within accessible cellular voids. These resin-rich regions are more directly exposed and engaged during indentation of the cross section, thereby increasing resistance to local penetration. In contrast, the response of the radial and tangential surfaces remains more strongly governed by the inherent organization of the wood structure and the local distribution of the polymer.

The flexural strength increased with WEP concentration and reached 115 MPa at 25% WEP, representing an improvement of 29% compared with the 0% WEP (Fig. 3b). The mechanical enhancement can be attributed to the combined effects of resin retention, local reinforcement of cellular structures, and improved load transfer across structurally weak regions. The cured WEP associated with cell wall surfaces, pits, and locally filled lumina may reduce stress concentration around anatomical discontinuities and resist local deformation during bending. Previous studies on WEP-impregnated wood have reported improvements in mechanical properties after the formation of cured polymer phases within the wood structure (Hao et al. 2022; Sun et al. 2021). More generally, polymer occupation of accessible wood voids can contribute to reinforcement while preserving the hierarchical wood framework.

The surface wettability was also altered by WEP modification. The water contact angle increased from approximately 102° for the 0% WEP to 112° after treatment with 5% WEP (Fig. 3c), demonstrating reduced surface wettability. However, further increases in WEP concentration from 5% to 25% produced only limited additional changes in the contact angle. This plateau suggests that a relatively small amount of WEP was sufficient to modify the chemical character of the outermost surface detected by the water droplet, whereas further increases in bulk resin uptake primarily affected the internal wood structure rather than producing a proportional change in the macroscopic surface contact angle. The contact angle is also influenced by surface roughness and chemical heterogeneity; therefore, its response does not necessarily scale directly with total WPG.

The appearance of the specimens changed after WEP modification, as reflected by the color-difference results in Fig. 3d. The modified wood became darker than the unmodified wood, whereas the additional variation among the higher WEP concentrations was limited. Because all treatment groups were subjected to the same high-temperature curing procedure, the additional concentration-dependent color variation can primarily be associated with the increasing contribution of cured WEP and interactions between the resin and wood components during thermal treatment. The apparent plateau in both water contact angle and color difference further indicates that the outermost surface response reached a relatively stable state at lower WEP contents, even though WPG, density, and flexural strength continued to increase with WEP concentration.

Overall, the results in Fig. 3 show that the effects of WEP modification were strongly scale- and location-dependent. Surface-sensitive properties such as water contact angle approached a plateau at relatively low WEP concentration, whereas bulk properties such as flexural strength and cross-sectional hardness continued to increase as greater quantities of WEP were retained within the wood. This distinction is consistent with a heterogeneous distribution of the resin between the outer surface and the internal cellular structure.

Chemical reactivity and thermal stability

The curing behavior of WEP and the chemical changes associated with wood modification were first examined by FTIR spectroscopy (Fig. 4a). The characteristic absorption at 913 cm^{-1}, assigned to the epoxy group of uncured WEP, disappeared after curing at 170°C. Meanwhile, changes in the broad band near 3372 cm^{-1} and in the region of 1100 – 1030 cm^{-1} were observed after curing. These changes are consistent with consumption of epoxy functionalities and formation of the cured epoxy network (Chen et al. 2024; Wang et al. 2021).

The FTIR spectra of the wood specimens retained the characteristic bands of lignocellulosic materials (Fig. 4b). The broad band at 3333 cm^{-1} is associated mainly with O-H stretching, whereas bands near 2919 and 2884 cm^{-1} arise from C-H stretching vibrations. The absorption around 1730 cm^{-1} is associated with carbonyl-containing structures, particularly those in hemicellulose and lignin, while the band near 1592 cm^{-1} is related to aromatic structures. With increasing WEP concentration, changes in

the relative intensity of these bands were accompanied by an increasing contribution near 829 cm^{-1}, associated with the substituted aromatic structure of WEP (Bi et al. 2022; Zhang et al. 2024). These spectral changes demonstrate the increasing contribution of the cured WEP to the chemical composition of the modified wood.

The thermal behavior of the specimens is shown in Fig. 4c. Compared with the 0% WEP, the temperatures associated with water removal and the principal degradation stages shifted to higher values after WEP modification. The temperatures corresponding to water evaporation ($T_{\mathrm{H_2O}}$), the first maximum degradation temperature (T_{max1}), and the second maximum degradation temperature (T_{max2}) generally increased with WEP concentration, while the residual mass at 600°C (W_R-600) also increased. These results indicate that incorporation of the cured WEP altered the thermal degradation behavior and enhanced the overall thermal stability of the modified wood. Similar improvements in thermal stability have been reported for wood containing in situ cured WEP or WEP-based modification systems (Hao et al. 2022; Sun et al. 2021; Wang et al. 2021). The enhanced thermal stability can be related to the formation of a thermoset polymer phase within the wood structure and to interactions between the cured resin and the lignocellulosic matrix (Wang et al. 2021). The increased residual mass further suggests that modification altered the decomposition pathway and/or promoted formation of a more thermally persistent residue.

The XRD patterns are shown in Fig. 4d. The characteristic diffraction of cellulose was retained after WEP modification, and no new sharp diffraction peaks appeared with increasing WEP concentration. This indicates that WEP modification did not change the basic crystalline form of the cellulose component. The cured WEP is predominantly non-crystalline and therefore mainly contributed to the amorphous region rather than producing new crystalline reflections. Consequently, the major performance improvements observed in Figs. 1–3 are more reasonably associated with resin uptake, curing, distribution, and interfacial interactions than with a transformation of the cellulose crystalline structure. Because a quantitative crystallinity index was not reported, changes in peak intensity alone should not be interpreted as a quantitative increase or decrease in cellulose crystallinity.

XPS analysis was further performed to investigate the changes in the chemical composition of wood induced by WEP modification (Fig. 5). The high-resolution C 1s spectra could be deconvoluted into three major components centered at approximately 284.86, 286.36, and 288.46 eV. The peak at approximately 284.86 eV was assigned mainly to C-C/C-H bonds associated with non-oxygenated aliphatic and aromatic carbon, whereas the component at approximately 286.36 eV was attributed primarily to C-O bonds in hydroxyl and ether groups. The higher-binding-energy component at approximately 288.46 eV was associated with highly oxidized carbon species, such as O-C = O groups. Similar assignments have been widely used for the analysis of wood and lignocellulosic surfaces by XPS (Sun et al. 2021; Wang et al. 2021). Compared with unmodified wood, the relative contribution of the C-C/C-H component became more pronounced, particularly at WEP concentrations of 15% and 25%, whereas the contribution of oxygen-containing carbon environments decreased. This change is consistent with the increasing

contribution of the cured epoxy network, which contains abundant aromatic and aliphatic carbon structures, to the outermost region of the modified wood (Sun et al. 2021).

The elemental compositions in Table 1 further demonstrate that the chemical changes were dependent on both WEP concentration and sampling position. The surface O/C atomic ratio calculated from the XPS data was 0.25 for unmodified wood, increased to 0.32 at 5% WEP, and then both decreased to 0.21 at 15% and 25% WEP. Because XPS is highly surface-sensitive, these variations reflect changes in the chemical composition of the outermost region rather than the bulk composition of the wood. The initial increase in the O/C ratio at 5% WEP suggests that, at a relatively low resin concentration, the wood surface was not yet covered by a continuous resin-rich phase and remained dominated by exposed oxygen-containing groups originating from wood carbohydrates and the oxygen-containing moieties of WEP. In contrast, the substantially lower O/C ratios at 15% and 25% WEP indicate increasing enrichment of carbon-rich cured WEP at the wood surface. The corresponding increase in the C 1s contribution at 284.8 eV in Fig. 5 supports this interpretation. Previous XPS studies have shown that the O/C ratio and the relative contributions of the deconvoluted C 1s components are sensitive indicators of changes in the surface composition of wood, although their interpretation must account for the heterogeneous distribution of lignin, carbohydrates, extractives, and introduced polymers (Hao et al. 2022; Sun et al. 2021; Wang et al. 2021).

Table 1
Surface and interior elemental compositions and O/C atomic ratios of unmodified and WEP-modified wood determined by XPS.

WEP Conc. /%	Surface C /%	Surface O /%	Surface O/C	Interior C /%	Interior O /%	Interior O/C
0	79.92	20.08	0.25	73.05	26.95	0.37
5	76.06	23.94	0.32	79.32	20.68	0.26
15	83.07	16.93	0.21	73.19	26.81	0.37
25	82.68	17.32	0.21	73.71	26.29	0.36

A different trend was observed in the interior of the samples. The interior O/C ratio decreased from 0.37 for unmodified wood to 0.26 for 5% WEP treated wood, indicating pronounced carbon enrichment within the investigated interior region. However, the O/C ratios of the 15% and 25% WEP-modified samples were 0.37 and 0.36, respectively, close to that of unmodified wood. This result should not be interpreted as an absence of WEP in the interior because XPS probes only a nanometer-scale surface region of the particular area exposed for analysis, whereas resin distribution within the heterogeneous wood cellular structure is spatially non-uniform. Rather, the results suggest a concentration-dependent balance between penetration and local accumulation. The 5% WEP could more readily access internal wood pores and exposed cell-wall regions, producing a distinct change in the local interior surface composition. Whereas, increasing WEP concentration promoted a greater overall resin uptake, as demonstrated by the continuously increasing WPG and density in Fig. 1, but also enhanced resin

accumulation in surface and near-surface regions. At higher concentrations, the freshly exposed interior area analyzed by XPS could therefore remain locally dominated by native wood components even though WEP was present elsewhere in the cell walls, pits, vessels, and other anatomical voids. This interpretation is consistent with previous studies showing that microwave-assisted impregnation can improve wood permeability and that in situ cross-linking of WEP within wood can increase resin retention and improve dimensional, mechanical, and thermal properties (Terziev et al. 2020; Wang et al. 2018).

The progressive increase in WPG and density with WEP concentration indicates increasing resin retention, while the decrease in water absorption and swelling and the increase in anti-swelling efficiency demonstrate that the introduced WEP restricted water-accessible pathways and the moisture-induced deformation of the wood structure. Meanwhile, the increase in flexural strength and cross-sectional hardness suggests that the cured resin contributed to reinforcement of the internal cellular structure. Thus, the XPS results, together with the FTIR results in Fig. 4 and the subsequent SEM observations, support a modification mechanism involving both chemical changes at the wood-WEP interface and physical occupation of accessible wood microstructures by the cured resin network. Previous studies on WEP-modified wood similarly reported that in situ cross-linking of epoxy-based networks within the wood structure improved dimensional stability, water resistance, thermal stability, and mechanical performance (Terziev et al. 2020; Wang et al. 2018).

Micromorphology analysis

The microstructures of the 0% WEP-treated and WEP-modified wood are shown in Fig. 6. The 0% WEP modified wood retained the characteristic porous cellular structure of aspen wood, with large vessel lumina and surrounding smaller cellular pores remaining predominantly open (Fig. 6a). The lumen-facing surfaces indicated by the yellow arrows showed no obvious resin deposits. Local structural discontinuities and opened or damaged anatomical features were observed in the regions highlighted by the red ellipses. Because the 0% WEP modified wood underwent the same ultrasonic-microwave treatment as the WEP-containing groups, these features may be associated, at least in part, with the physical treatment process.

Microwave treatment of moist wood can generate rapid internal heating and vapor-pressure gradients, and sufficiently intensive treatment has been reported to disrupt pit membranes, weak middle-lamella regions, rays, and other anatomical structures, thereby increasing wood permeability (Terziev et al. 2020). Ultrasound can additionally promote liquid movement and mass transfer through acoustic agitation and cavitation-related effects (Wang et al. 2018). These mechanisms provide a plausible basis for the formation or opening of accessible transport pathways during the combined treatment. After impregnation with 5% WEP, the overall cellular framework remained largely open, but smoother deposits became visible locally on lumen-facing surfaces (Fig. 6b). The region indicated by the yellow arrow shows a rougher internal surface than that of the 0% WEP, suggesting deposition of a relatively thin and discontinuous WEP-rich phase. At the same time, the pit-related openings and other anatomical pathways highlighted by the red ellipses remained largely accessible rather than being completely

blocked. This morphology is consistent with the comparatively moderate WPG and density at 5% WEP and with the XPS results, which revealed a pronounced change in the chemical composition of the investigated interior region without the strong carbon enrichment observed at the outer surfaces of the higher-concentration specimens.

At 15% WEP, a more pronounced change in morphology was observed (Fig. 6c). More continuous resin-rich regions were present along lumen-facing surfaces, as indicated by the yellow arrows, while the enlarged region highlighted in the red ellipse showed a film-like polymer phase locally associated with the internal wood surface. At this concentration, the resin was no longer present only as isolated local deposits but formed more continuous domains along some internal surfaces and within accessible void regions. Epoxy-impregnated wood systems have similarly been reported to form continuous polymer phases associated with the cellular wood structure (Zhang et al. 2020). At 25% WEP, extensive local accumulation of cured resin was evident (Fig. 6d). Smooth resin-rich regions occupied smaller cellular spaces (red ellipse) and, in some locations, partially or nearly completely filled larger lumina (yellow arrow). Nevertheless, open lumina were still present, demonstrating that WEP distribution remained heterogeneous rather than producing complete and uniform filling of the wood structure. Such heterogeneity is expected because the dimensions, connectivity, and accessibility of vessels, pits, and other anatomical pathways vary spatially within wood. Previous research has similarly shown that polymer incorporation into accessible wood voids can reinforce the cellular structure and improve dimensional or mechanical performance while retaining the underlying hierarchical wood architecture (Liu et al. 2020; Zhang et al. 2020).

The concentration-dependent microstructural evolution observed by SEM provides a direct morphological basis for the physical properties shown in Fig. 1. Increasing WEP concentration produced progressively greater deposition and local occupation of the cellular structure, resulting in higher WPG and density. The cured WEP reduced the effective volume and continuity of some capillary pathways available for liquid-water transport, thereby contributing to the decrease in water absorption. At the same time, the retained resin could restrict moisture-induced deformation of the surrounding wood structure, consistent with the lower swelling and shrinkage and higher anti-swelling and anti-shrinkage efficiencies shown in Fig. 2. Similar relationships between polymer retention within wood and improved water resistance and dimensional stability have been reported for WEP-modified wood (Sun et al. 2021; Wang et al. 2021).

The SEM observations also help explain the mechanical-property changes in Fig. 3. Increasing amounts of cured WEP associated with lumen surfaces and locally filled cellular regions could reinforce structurally weak regions, reduce local deformation, and facilitate stress transfer during bending. This interpretation is consistent with the progressive increase in flexural strength and the pronounced enhancement in cross-sectional hardness. The stronger response of cross-sectional hardness compared with radial and tangential hardness can be related to the longitudinal organization of the wood cellular structure and the direct exposure of resin-associated lumina and internal surfaces on the cross section.

Overall, the SEM results reveal a concentration-dependent transition from a predominantly open cellular structure to one containing increasingly continuous WEP-rich layers and locally resin-filled regions. Combined with the FTIR and XPS results, these observations suggest that the improvement in wood performance arose from several coupled effects: transport of the aqueous WEP system through accessible anatomical pathways, retention and curing of WEP within the hierarchical wood structure, partial restriction of water-transport pathways, local reinforcement of cellular regions, and interfacial interactions between the cured resin and wood components. Thus, the ultrasonic-microwave-assisted process provided an effective route for incorporating a waterborne thermosetting resin into wood, while the WEP concentration governed the extent and spatial characteristics of the retained polymer phase.

Conclusions

This study developed an efficient and environmentally oriented wood modification strategy by combining ultrasonic-microwave synergistic impregnation with waterborne epoxy resin (WEP). The synergistic treatment facilitated the transport and distribution of the aqueous WEP system within the hierarchical porous structure of wood, while the use of WEP reduced reliance on organic-solvent-based modifiers and provided a lower-VOC modification route. Increasing the WEP concentration progressively enhanced resin retention and improved wood performance. At 25% WEP, the weight percent gain reached approximately 39% and the density increased from 0.41 to 0.49 g/cm³. Meanwhile, water absorption and dimensional changes were substantially reduced, with maximum decreases of approximately 45% in radial swelling and 30% in tangential shrinkage. The flexural strength increased to 115 MPa, representing an improvement of approximately 29% compared with unmodified wood, while cross-sectional hardness and surface hydrophobicity were also enhanced.

The improved performance resulted from the combined effects of enhanced impregnation through accessible anatomical pathways, in situ curing and retention of WEP within the wood structure, partial occupation of water-transport pathways, and interfacial interactions between the cured resin and wood components. Overall, the coupling of ultrasonic-microwave process intensification with an aqueous epoxy resin system provides a promising approach for improving both the efficiency and environmental compatibility of wood modification and offers potential for the development of durable, high-performance wood products.

Declarations

Conflict of interest statement

The authors declare that they have no conflicts of interest regarding this article.

Funding

This work was financially supported by grant from the National Key Research and Development Program of China (2024YFD2201502).

Author Contribution

Xinhao Feng and Yuehan Sun: Writing-original draft. Tingting Peng and Zhaozhe Yang: Software, Data curation. Jian Chen and Guomin Wu: Software, Data curation, Validation. Xinhao Feng, Zhaozhe Yang, and Zhihui Wu: Writing-review & editing, Validation, Supervision, Funding acquisition.

Acknowledgement

This research was started by undergraduates of Xuan Zhuang and Xiyue Zhao at January 2023, and the WEP was synthesized and provided by Prof. Jian Chen and Guomin Wu from Institute of Chemical Industry of Forest Product. We are grateful for their efforts and supports.

References

1. Bastani A, Adamopoulos S, Militz H (2015) Water uptake and wetting behaviour of furfurylated, N-methylol melamine modified and heat-treated wood. Eur J Wood Wood Prod 73:627–634. http://doi.org/10.1007/s00107-015-0919-8
2. Bi Z, Morrell JJ, Lei Y, Yan L, Ji M (2022) Eco-friendly and mildly modification of wood cell walls with heat treated wood extracts to improve wood decay resistance. Ind Crops Prod 184:115079. http://doi.org/https://doi.org/10.1016/j.indcrop.2022.115079
3. Brischke C, Alfredsen G (2020) Wood-water relationships and their role for wood susceptibility to fungal decay. Appl Microbiol Biotechnol 104:3781–3795. http://doi.org/10.1007/s00253-020-10479-1
4. Chang HT, Chang ST (2002) Moisture excluding efficiency and dimensional stability of wood improved by acylation. Bioresour Technol 85:201–204. http://doi.org/10.1016/s0960-8524(02)00085-8
5. Chen C, Pan J, Xu H, Han S, Xiao J, Ren X, Wang H, Wu X, Zhang Y, Sun F (2024) Wood composites with enhanced dimensional stability and decay resistance fabricated by in-situ curing of waterborne epoxy resin containing tertiary amine cation. Constr Build Mater 457. http://doi.org/10.1016/j.conbuildmat.2024.139420
6. Digaitis R, Thybring EE, Thygesen LG, Fredriksson M (2021) Targeted acetylation of wood: a tool for tuning wood-water interactions. Cellulose 28:8009–8025. http://doi.org/10.1007/s10570-021-04033-z
7. Dong YM, Yan YT, Wang KL, Li JZ, Zhang SF, Xia CL, Shi SQ, Cai LP (2016) Improvement of water resistance, dimensional stability, and mechanical properties of poplar wood by rosin impregnation. Eur J Wood Wood Prod 74:177–184. http://doi.org/10.1007/s00107-015-0998-6

8. Elaieb MT, Shel F, Jalleli M, Langbour P, Candelier K (2019) Physical properties of four ring-porous hardwood species: influence of wood rays on tangential and radial wood shrinkage. Madera Y Bosques 25:e2521695. http://doi.org/10.21829/myb.2019.2521695
9. Flores EMM, Cravotto G, Bizzi CA, Santos D, Iop GD (2021) Ultrasound-assisted biomass valorization to industrial interesting products: state-of-the-art, perspectives and challenges. Ultrason Sonochem 72:1–12. http://doi.org/10.1016/j.ultsonch.2020.105455
10. Hao XH, Li ML, Huang YS, Sun YH, Zhang KX, Guo CG (2022) High-Strength, Dimensionally Stable, and Flame-Retardant Fast-Growing Poplar Prepared by Ammonium Polyphosphate-Waterborne Epoxy Impregnation. ACS Appl Polym Mater 4:1305–1313. http://doi.org/10.1021/acsapm.1c01712
11. He S, Lin LY, Fu F, Zhou YD, Fan MZ (2014) Microwave Treatment for Enhancing the Liquid Permeability of Chinese Fir. BioResources 9:1924–1938. http://doi.org/10.15376/biores.9.2.1924-1938
12. Huang YG, Li GY, Chu FX (2019) Modification of wood cell wall with water-soluble vinyl monomer to improve dimensional stability and its mechanism. Wood Sci Technol 53:1051–1060. http://doi.org/10.1007/s00226-019-01112-0
13. Hunt RWG (2002) Application of a model of color appearance to practical problems in imaging. Proc IEEE 90:57–63. http://doi.org/10.1109/5.982405
14. Li R, Sun F, Wang W, Tang J, Peng H, Li Z, Jiang J, Zhan T, Cai L, Lyu J (2025) Effect of delignification on shrinking and swelling of poplar wood assessed using digital image correlation technique. Int J Biol Macromol 289:138851. http://doi.org/10.1016/j.ijbiomac.2024.138851
15. Liu MH, Guo F, Wang HK, Ren WT, Cao MD, Yu Y (2020) Highly Stable Wood Material with Low Resin Consumption via Vapor Phase Furfurylation in Cell Walls. ACS Sustainable Chem Eng 8:13924–13933. http://doi.org/10.1021/acssuschemeng.0c03172
16. Liu Y, Hu JH, Gao JM, Guo HW, Chen Y, Cheng QZ, Via BK (2015) Wood Veneer Dyeing Enhancement by Ultrasonic-assisted Treatment. BioResources 10:1198–1212
17. Lu ZX, Wu ZG, Fan LW, Zhang H, Liao YQ, Zheng DY, Wang SQ (2016) Rapid and solvent-saving liquefaction of woody biomass using microwave-ultrasonic assisted technology. Bioresour Technol 199:423–426. http://doi.org/10.1016/j.biortech.2015.09.048
18. Mantanis GI (2017) Chemical Modification of Wood by Acetylation or Furfurylation: A Review of the Present Scaled-up Technologies. BioResources 12:4478–4489. http://doi.org/10.15376/biores.12.2.4478-4489
19. Roffael E (2016) Significance of wood extractives for wood bonding. Appl Microbiol Biotechnol 100:1589–1596. http://doi.org/10.1007/s00253-015-7207-8
20. Sandberg D, Kutnar A, Mantanis G (2017) Wood modification technologies - a review. IFOREST 10:895–908. http://doi.org/10.3832/ifor2380-010
21. Sun ZY, Lv JX, Wang ZH, Wu YQ, Yuan GM, Zuo YF (2021) Sodium silicate/waterborne epoxy resin hybrid-modified Chinese fir wood. Wood Sci Technol 55:837–855. http://doi.org/10.1007/s00226-021-01287-5

22. Terziev N, Daniel G, Torgovnikov G, Vinden P (2020) Effect of Microwave Treatment on the Wood Structure o Norway Spruce and Radiata Pine. BioResources 15:5616–5626. http://doi.org/10.15376/biores.15.3.5616-5626
23. Thybring EE, Kymäläinen M, Rautkari L (2018) Experimental techniques for characterising water in wood covering the range from dry to fully water-saturated. Wood Sci Technol 52:297–329. http://doi.org/10.1007/s00226-017-0977-7
24. Wang DY, Ling QH, Nie YJ, Zhang Y, Zhang WH, Wang H, Sun FL (2021) In-Situ Cross-Linking of Waterborne Epoxy Resin Inside Wood for Enhancing Its Dimensional Stability, Thermal Stability, and Decay Resistance. ACS Appl Polym Mater 3:6265–6273. http://doi.org/10.1021/acsapm.1c01070
25. Wang XQ, Yu ZM, Zhang Y, Qi CS, Chang WL (2018) Evaluation of ultrasonic-assisted dyeing properties of fast-growing poplar wood treated by reactive dye based on grey system theory analysis. J Wood Sci 64:861–871. http://doi.org/10.1007/s10086-018-1768-y
26. Weng X, Zhou YD, Fu ZY, Gao X, Zhou F, Jiang JH (2021) Effects of microwave pretreatment on drying of 50 mm-thickness Chinese fir lumber. J Wood Sci 67:1–9. http://doi.org/10.1186/s10086-021-01942-2
27. Xie YJ, Fu QL, Wang QW, Xiao ZF, Militz H (2013) Effects of chemical modification on the mechanical properties of wood. Eur J Wood Wood Prod 71:401–416. http://doi.org/10.1007/s00107-013-0693-4
28. Xu K, Wang Y, Lv JX, Li XJ, Wu YQ (2015) The Effect of Microwave Pretreatment on the Impregnation of Poplar Wood. BioResources 10:282–289. http://doi.org/10.15376/biores.10.1.282-289
29. Yang TT, Cao JZ, Ma EN (2019) How does delignification influence the furfurylation of wood? Ind Crops Prod 135:91–98. http://doi.org/10.1016/j.indcrop.2019.04.019
30. Yang Z, Chen J, Zhan X, Wu G, Kong Z (2024) A novel wood fiber/waterborne epoxy resin composite with high fiber content and performance fabricated by a green and simple process. Polym Compos 45:1898–1909. http://doi.org/10.1002/pc.27897
31. Zelinka SL, Altgen M, Emmerich L, Guigo N, Keplinger T, Kymäläinen M, Thybring EE, Thygesen LG (2022) Review of Wood Modification and Wood Functionalization Technologies. Forests 13:1–46. http://doi.org/10.3390/f13071004
32. Zhang LM, Wang A, Zhu TL, Chen Z, Wu YP, Gao YF (2020) Transparent Wood Composites Fabricated by Impregnation of Epoxy Resin and W-Doped VO2 Nanoparticles for Application in Energy-Saving Windows. ACS Appl Mater Interfaces 12:34777–34783. http://doi.org/10.1021/acsami.0c06494
33. Zhang T, Tan J, Li S (2024) Functional cellulose-derived epoxy cross-linked with BADGE resin to construct high-performance epoxy composites. Int J Biol Macromol 265:130569. http://doi.org/https://doi.org/10.1016/j.ijbiomac.2024.130569

Figures

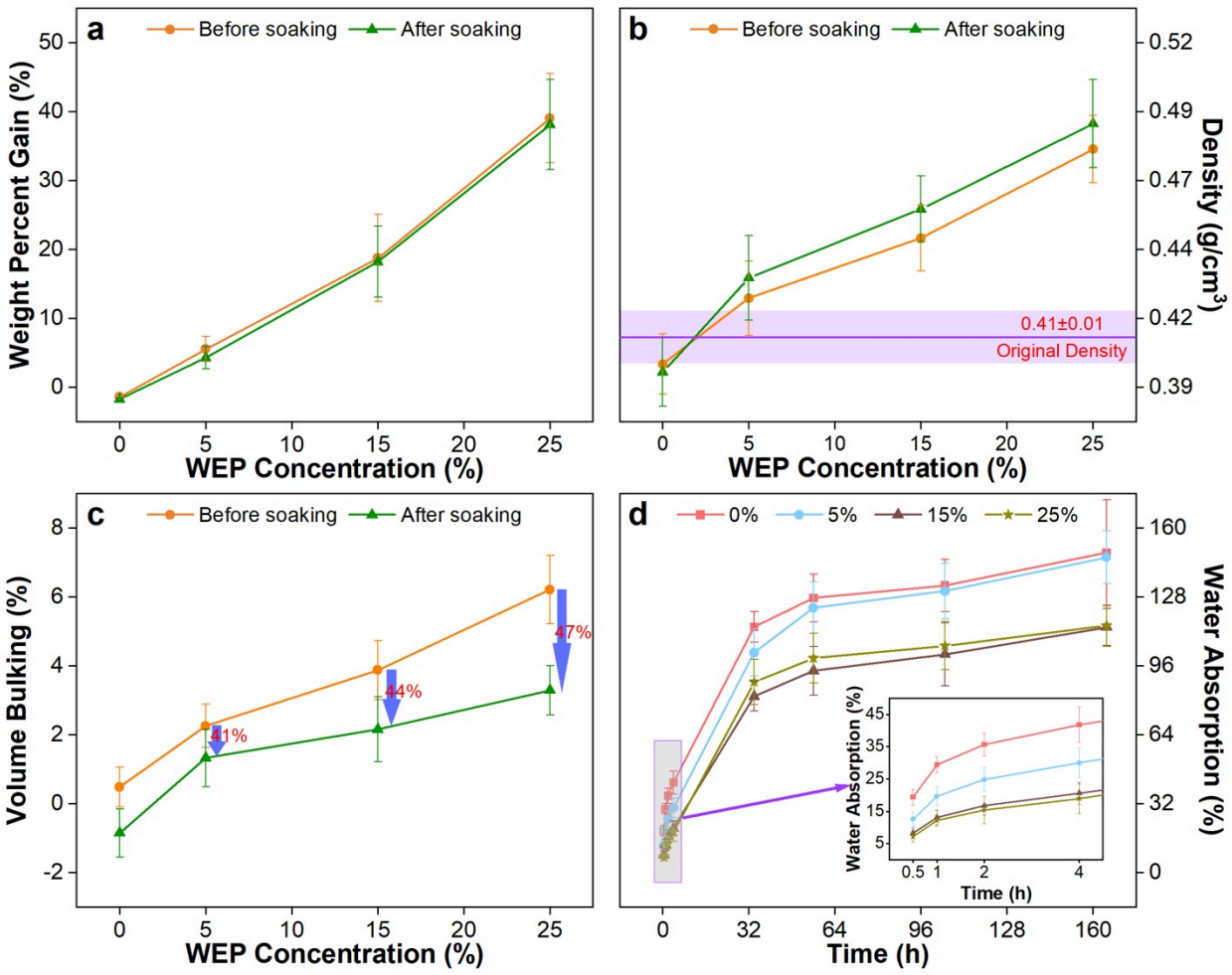


Figure 1

WPG (a), density (b), and volume bulking (c) of unmodified and modified wood before and after water soaking; the water absorption of modified wood with various times of water soaking (d).

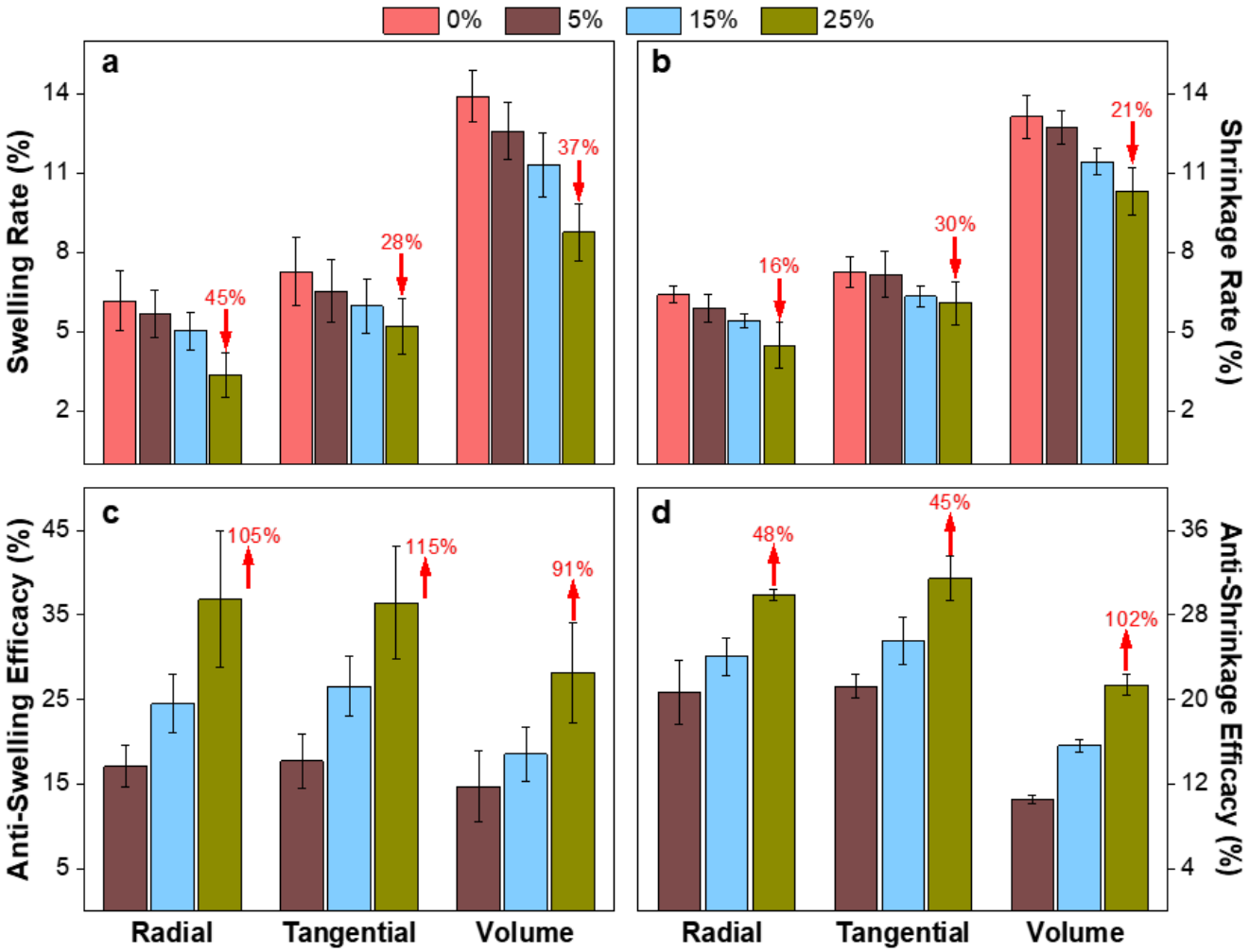


Figure 2

Swelling (a) and shrinkage (b) rate of unmodified and modified wood after water saturation and drying, respectively; anti-swelling (c) and anti-shrinkage (d) efficacy of modified wood at radial, tangential, and volume direction of wood.

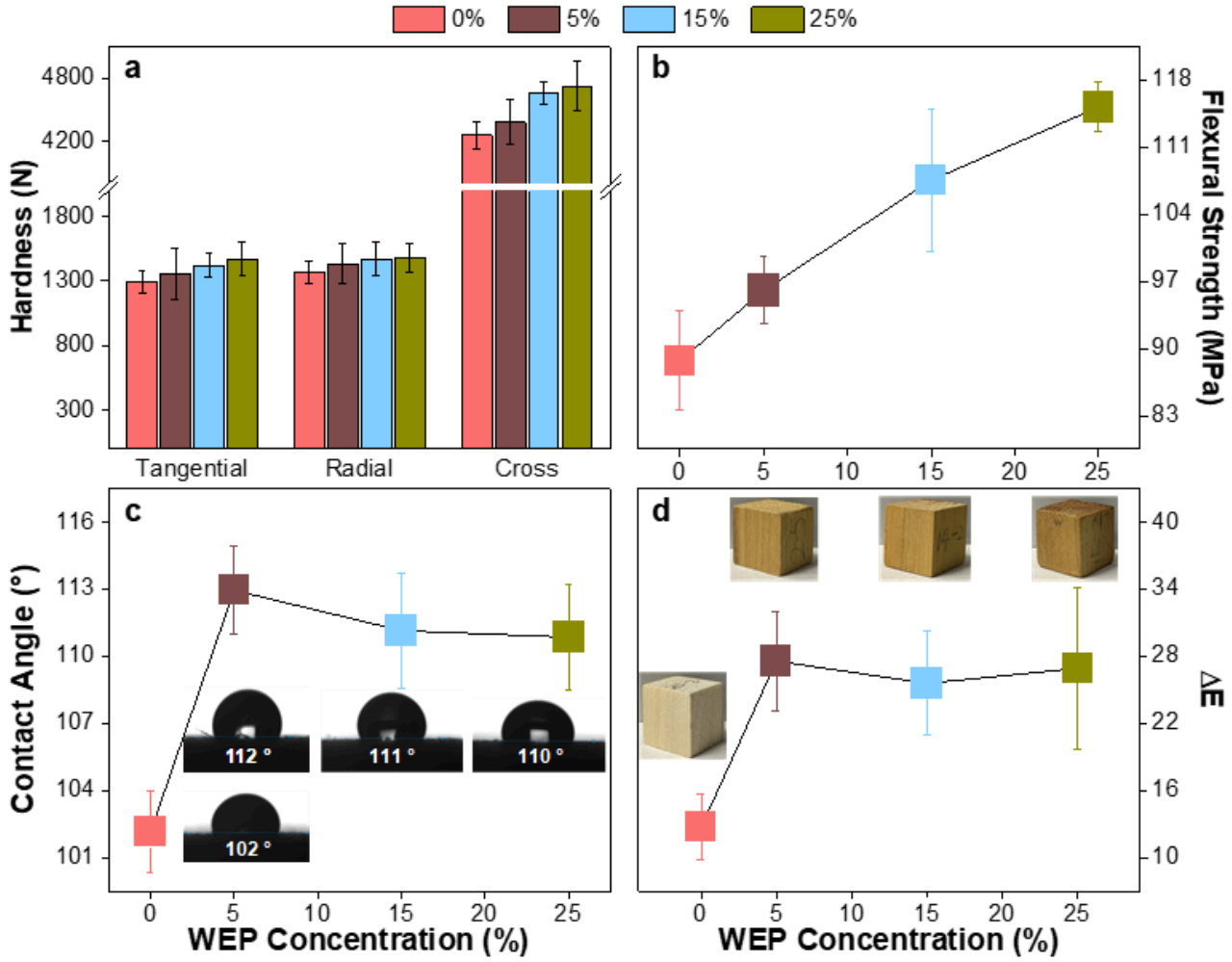


Figure 3

The hardness (a), flexural strength (b), water contact angle (c), and surface chromatic aberration (d) of wood modified with various WEP concentrations.

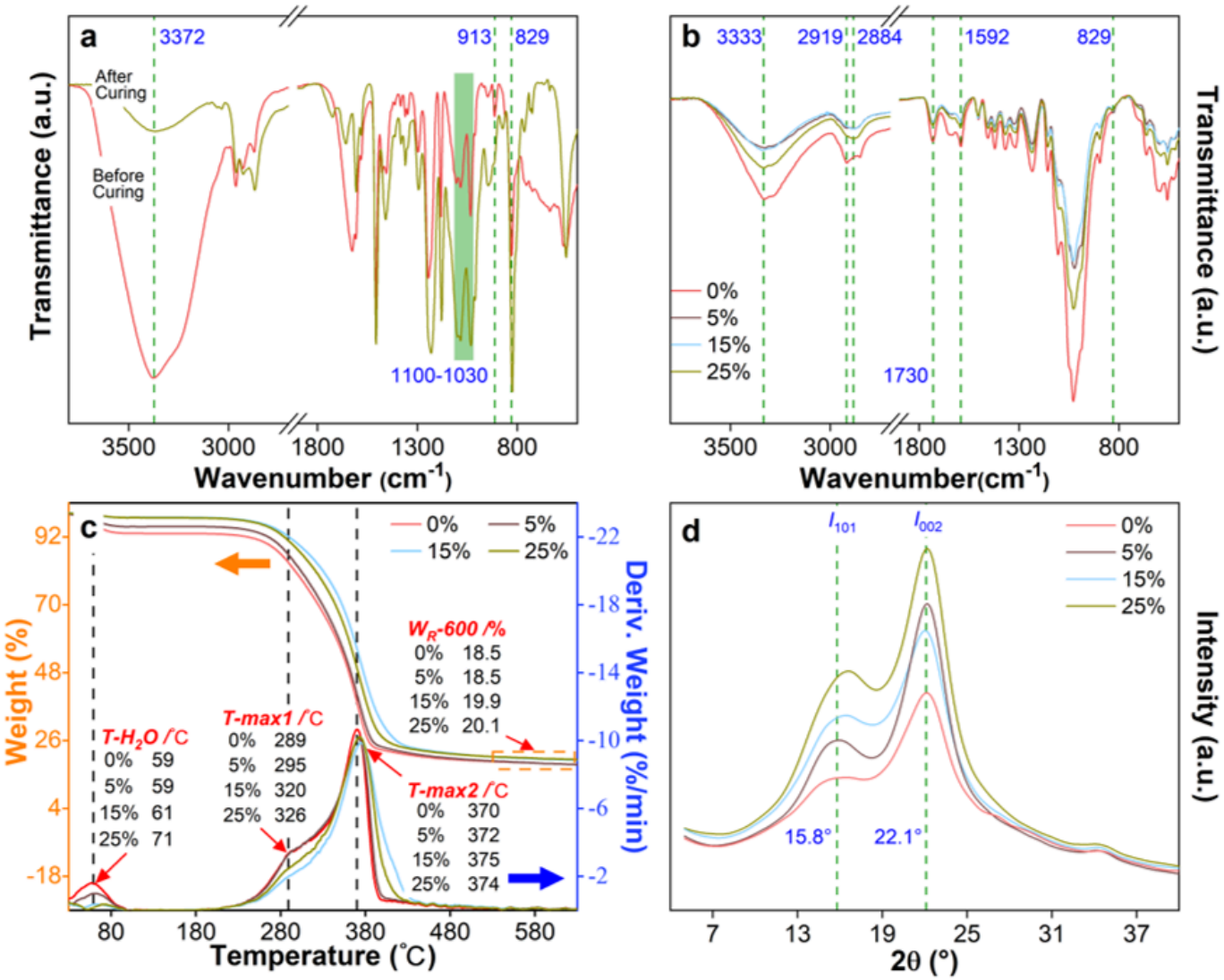


Figure 4

The FTIR of WEP before and after curing (a), and of wood modified with various WEP concentrations (b); the thermal stability (c) and crystallization behavior (d) of unmodified and modified wood measured by TG/DTG and XRD, respectively.

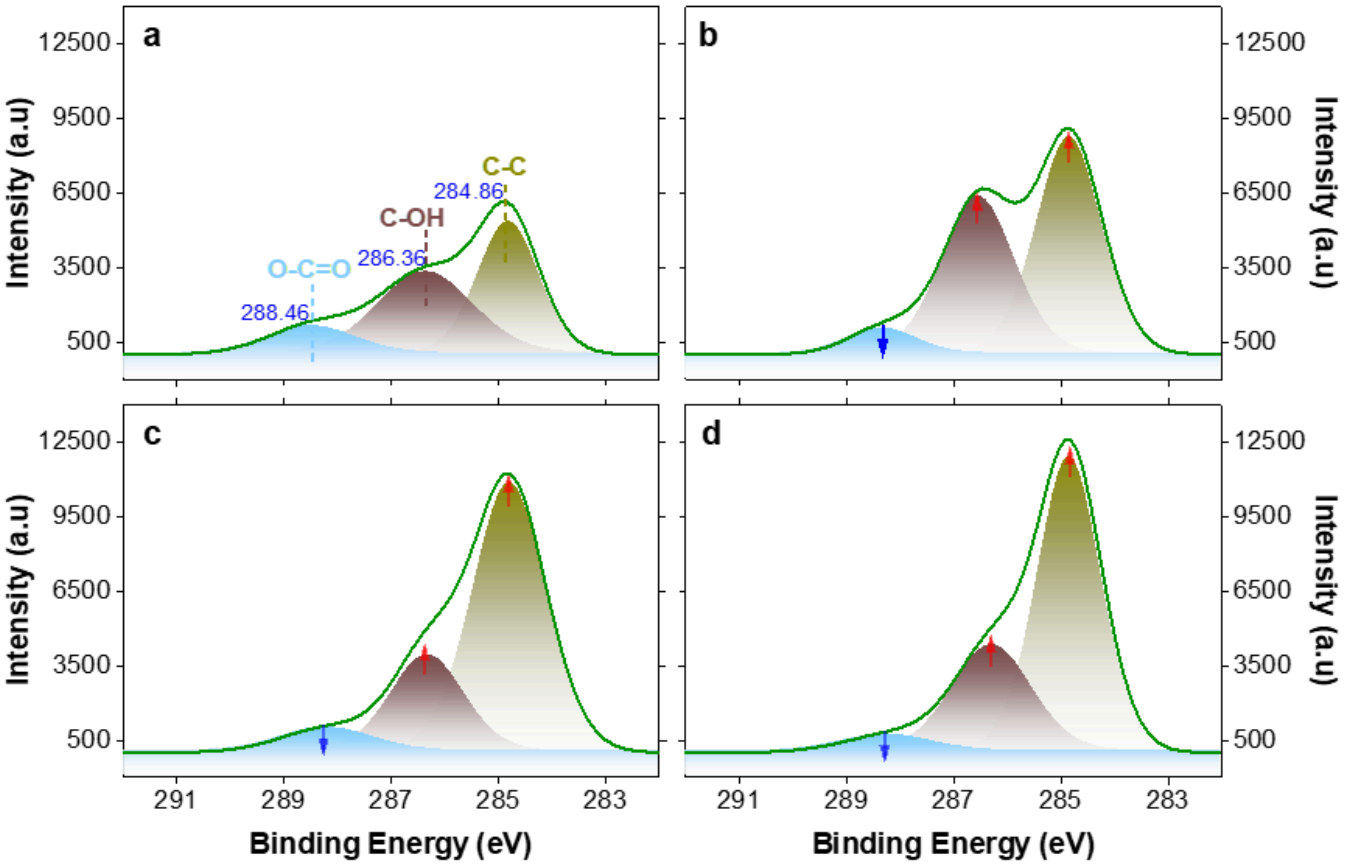


Figure 5

High-resolution C 1s XPS spectra and peak deconvolution of wood modified with WEP at concentrations of 0% (a), 5% (b), 15% (c), and 25% (d).

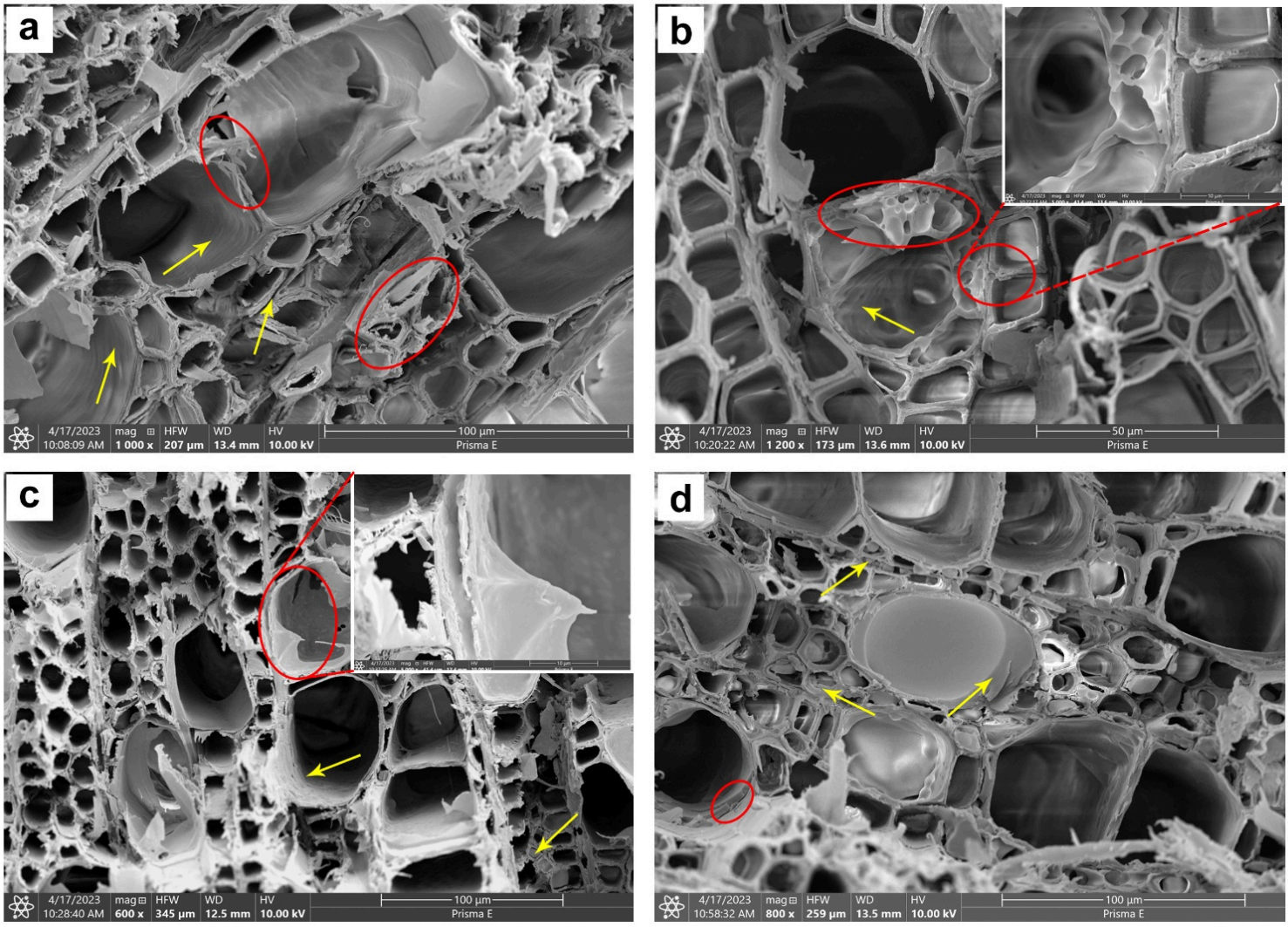


Figure 6

SEM images showing the micromorphology of wood treated with WEP concentrations of 0% (a), 5% (b), 15% (c), and 25% (d).